NEURAL REGENERATION RESEARCH
Volume 8, Issue 33, November 2013

www.nrronline.org

doi:10.3969/j.issn.1673-5374.2013.33.010 [http://www.nrronline.org; http://www.sjzsyj.org]

Tian X, Liu HJ, Geng ZJ, Yang H, Wang GS, Yang JP, Wang CX, Li CN, Li Y. Scanning pattern of diffusion tensor tractography and an analysis of the morphology and function of spinal nerve roots. Neural Regen Res. 2013;8(33):3159-3166.

Scanning pattern of diffusion tensor tractography and an analysis of the morphology and function of spinal nerve roots

Xin Tian, Huaijun Liu, Zuojun Geng, Hua Yang, Guoshi Wang, Jiping Yang, Chunxia Wang, Cuining Li, Ying Li

Department of Medical Imaging, the Second Hospital of Hebei Medical University, Shijiazhuang 050000, Hebei Province, China

Graphical Abstract

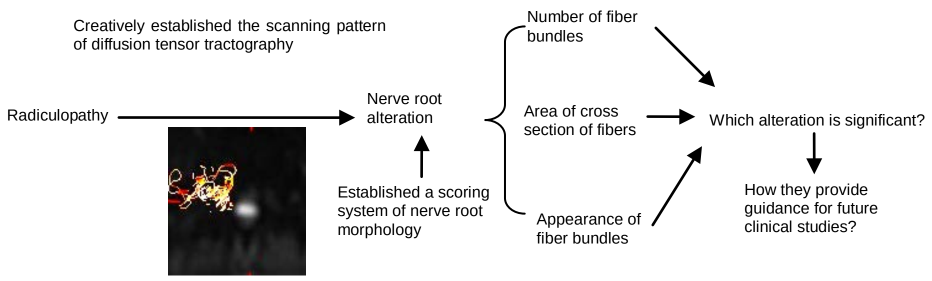

Xin Tian, M.D., Attending physician.

Corresponding author: Huaijun Liu, M.D., Doctoral supervisor, Professor, Chief physician, Department of Medical Imaging, the Second Hospital of Hebei Medical University, Shijiazhuang 050000, Hebei Province, China, huaijunliu@yahoo.com.cn; tellytianxin@gmail.com.

Received: 2013-06-08
Accepted: 2013-09-22
(N201303079)

Acknowledgments: We are very grateful to all teachers from the Technique Team, Department of Nuclear Magnetic Resonance, the Second Hospital of Hebei Medical University, China for their help in scanning.

Funding: This study was supported by the Instruction Project of Health Department of Hebei Province of China in 2012, No. 20120072.

Author contributions: Tian X participated in data analysis, manuscript writing, and obtaining funding. Liu HJ was in charge of study concept and design, and served as the principle investigator. Geng ZJ, Yang H, Wang GS, Yang JP, Wang CX, Li CN, and Li Y participated in statistical processing and literature retrieval. All authors approved the final version of the paper.

Abstract

Radiculopathy, commonly induced by intervertebral disk bulging or protrusion, is presently diagnosed in accordance with clinical symptoms because there is no objective quantitative diagnostic criterion. Diffusion tensor magnetic resonance imaging and diffusion tensor tractography revealed the characterization of anisotropic diffusion and displayed the anatomic form of nerve root fibers. This study included 18 cases with intervertebral disc degeneration-induced unilateral radiculopathy. Magnetic resonance diffusion tensor imaging was creatively used to reveal the scanning pattern of fiber tracking of the spinal nerve root. A scoring system of nerve root morphology was used to quantitatively assess nerve root morphology and functional alteration after intervertebral disc degeneration. Results showed that after fiber tracking, compared with unaffected nerve root, fiber bundles gathered together and interrupted at the affected side. No significant alteration was detected in the number of fiber bundles, but the cross-sectional area of nerve root fibers was reduced. These results suggest that diffusion tensor magnetic resonance imaging-based tractography can be used to quantitatively evaluate nerve root function according to the area and morphology of fiber bundles of nerve roots.

Key Words

neural regeneration; spinal cord injury; magnetic resonance; diffusion imaging; tracking; nerve injury; nerve root; degenerative disease; grants-supported paper; neuroregeneration

Conflicts of interest: None declared.

Ethical approval: This study was approved by the Ethics Committee, the Second Hospital of Hebei Medical University, China.

Author statements: The manuscript is original, has not been submitted to or is not under consideration by another publication, has not been previously published in any language or any form, including electronic, and contains no disclosure of confidential information or authorship/patent application/funding source disputations.

INTRODUCTION

Nearly two-thirds of adults suffer from low back pain[1]. Axial spine pain is frequently accompanied with nerve root pain or radiculopathy. Patients often experience pain from the buttocks to the leg and foot along the back of thigh, sometimes accompanying reduced muscle strength. Under the above-mentioned conditions, it is unclear whether the function of the nerve root is altered and what kind of change has occurred. In this study, we sought to understand and quantitatively analyze the function of spinal nerve roots in patients with radiculopathy.

In particular, we want to answer the following questions: (1) What degree and type of nerve root injury occurs in patients with radiculopathy? (2) What changes in morphology and function of nerve tracts occur after nerve root function is affected?

Radiculopathy refers to skin pain and paresthesia induced by spinal nerve root dysfunction, as well as muscle weakness and deep tendon reflex. The most common reason for radiculopathy is spinal disease and intervertebral disk bulging or protrusion[2]. Most lumbago is non-specific and cannot be diagnosed only by clinical symptoms. However, if the patients are affected with symptoms and signs of radiculopathy on the lumbar section, they should be questioned about their case history and subjected to physical examination[3]. Nevertheless, clinicians cannot judge the source and severity of radiculopathy merely by collecting the above-described data. In these incidences, imaging examination is necessary.

Radiography, CT and MRI can reveal spinal degeneration-induced radiculopathy. Radiography shows spinal degenerative changes and spinal stability[4]. However, radiography is unable to image the structure of soft tissue or nerve roots. CT apparently displays intervertebral disk bulging or protrusion and lateral recess narrowing[5], but CT examination requires a high radiation dose, and so cannot be used many times[6]. These examination methods cannot reveal nerve fibers after spinal nerve root injury. MRI can clearly reveal intervertebral disk bulging or protrusion, and directly display whether nerve root compression has occurred[7]. T2-weighted images (T2WI) can show the existence of epidural adipose capsule, intervertebral disc morphology and component[8]. T1-weighted images (T1WI) play an important role in the evaluation of nerve structure, intervertebral disc morphology and articular surface morphology[9].

Recently, some scholars have begun investigating dynamic MRI, and have measured and evaluated distance and angle of vertebral translational displacement on the central sagittal plane[10-11]. Dynamic MRI has revealed abnormal intervertebral disc morphology in patients with radiculopathy[10-11]. However, anatomical images obtained with MRI were not helpful for improving patient prognosis, only slightly affected the formulation of the therapeutic regimen[12], and had no role in judgment of prognosis[13-14]. With the development of MRI, besides conventional T1WI and T2WI sequences, fast imaging employing steady-state acquisition has been applied to obtain nerve root images[15]. Fast imaging employing steady- state acquisition has also been employed to perfectly reveal dorsal root ganglia of thoracic segments, and nerve roots and cauda equina nerves of the lumbar spine[16-18].

Functional MRI can evaluate the degree of nerve root injury at the molecular level. Diffusion tensor MRI (DT-MRI) and diffusion tensor tractography can sensitively detect molecular diffusion in a three-dimensional space, and reveal the characterization of anisotropic diffusion, the pathway of molecular diffusion, and completely exhibit the anatomical form of fiber bundles of nerve roots.

Currently, the diagnosis of radiculopathy remains based on clinical manifestations of the patients, because there is no quantitative index to judge whether nerve roots are affected or the severity of the change. This study first used diffusion tensor tractography to reveal radiculopathy by the following: (1) Optimization and implementation of scanning parameters of diffusion tensor imaging, and an image analysis index and method for spinal nerve root injury diagnosis. (2) Optimization of image post-processing of diffusion tensor tractography of the nerve root. (3) Summarize a quantitative evaluation system for determining the extent of nerve root injury.

RESULTS

Baseline data of subjects

A total of 18 patients with intervertebral disc degeneration-induced radiculopathy were included in this study (Table 1).

Table 1 Baseline data of patients with intervertebral disc degeneration-induced radiculopathy

No.	Gender	Age (year)	Side	Involved segment
1	Female	72	Right	L_5–S_1
2	Female	58	Left	$L_{4–5}$
3	Female	66	Right	$L_{4–5}$
4	Male	57	Right	$L_{4–5}$
5	Male	47	Right	L_5–S_1
6	Male	70	Left	$L_{4–5}$
7	Male	63	Right	L_5–S_1
8	Male	48	Left	L_5–S_1
9	Female	40	Left	$L_{4–5}$
10	Male	71	Right	L_5–S_1
11	Female	44	Right	L_5–S_1
12	Male	66	Right	L_5–S_1
13	Male	20	Left	$L_{4–5}$
14	Female	49	Right	$L_{4–5}$
15	Female	49	Right	L_5–S_1
16	Female	57	Left	$L_{4–5}$
17	Male	60	Right	L_5–S_1
18	Female	50	Left	L_5–S_1

Male-female ratio was 1:1; mean age of 53.3±13.3 years. There were 11 patients with right radiculopathy, and 7 patients with left radiculopathy.

MRI images revealed intervertebral disc degeneration, bulging or protrusion, resulting in intervertebral foramina narrowing, nerve root compression, accompanied by nerve root displacement or unclear boundaries between nerve roots and intervertebral discs (Figure 1). All 18 patients were included in the final analysis.

Comparison of the number of nerve root fibers between affected and unaffected sides in patients with intervertebral disc degeneration-induced radiculopathy

Volume one software was applied to calculate the number of fiber bundles. The number of fiber bundles ranged from 40 to 88, averaging 61.28 ± 11.13 on the unaffected side. The number of fiber bundles ranged from 29 to 84, averaging 57.11 ± 13.40 on the affected side. Both agreed with normal distribution ($F_{\text{unaffected side}}$ = 0.356 4, $F_{\text{affected side}}$ = 0.978 7). The number of fiber bundles on the unaffected side had a central tendency, mainly between 56 and 68, but the number of fiber bundles on the affected side had a scattered tendency, mainly between 51 and 67. The number of fiber bundles was lower on the affected side than that on the unaffected side, but no significant difference was detectable (P > 0.05).

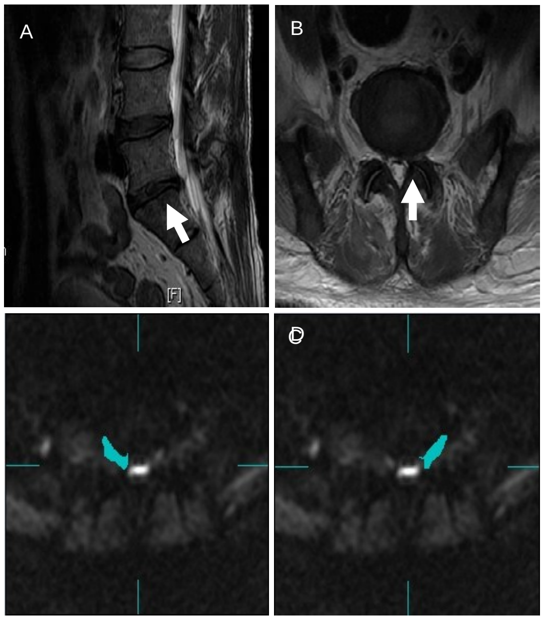

Figure 1 Magnetic resonance images of a 55-year-old male patient with intervertebral disc degeneration-induced radiculopathy.

He presented with left lower limb pain and weakness. (A) Lumbar sagittal T2-weighted images (T2WI). (B) L_5/S_1 axial T2WI. (C, D) Region of interest of the diffusion tensor tractography. The L_5/S_1 intervertebral disc appears black, and the protrusion is marked with the white arrow. The left intervertebral foramina was narrow and the left nerve root was compressed (A, B, arrow).

The boundary between the nerve root and the intervertebral disc was not visible. Bilateral intervertebral foramina were considered the region of interest to calculate the fiber bundle map, maintaining bilateral symmetry and identical area when drawing.

Comparison of the cross-sectional area of nerve root fibers between the affected and unaffected sides in patients with intervertebral disc degeneration-induced radiculopathy

Volume one software was used to perform image post-processing. The cross-sectional area of the nerve root fibers on the unaffected side ranged from 703 to 5 000/unit, averaging 2 100.67 ± 1 060.89/unit. The cross-sectional area of the nerve root fibers on the affected side ranged from 463 to 2 840/unit, averaging 1 356.11 ± 634.63/unit. There were significant differences in the cross-sectional area of the nerve root fibers between affected and unaffected sides, and the area was smaller on the affected side than on the unaffected side ($P < 0.05$).

Comparison of morphology of nerve root fibers between affected and unaffected sides in patients with intervertebral disc degeneration-induced radiculopathy

Morphological score of nerve root fibers according to integrity and branches is shown in Table 2.

Table 2 Scoring system for nerve root fiber morphology (points)

Item	With branches	Without branches
Intact	2	1
Incomplete	1	0

2 points: intact fiber bundle with clear branches; 0 point: incomplete fiber bundles, visible breakage, without branches.

On the unaffected side, one fiber scored 0 point (5.6%); six fibers scored 1 point (33.3%); 11 fibers scored 2 points (61.1%). On the affected side, five fibers scored 0 point (27.8%), 12 fibers scored 1 point (66.7%), and one fiber scored 2 points (5.6%). On the unaffected side, most fibers scored 2 points; but on the affected side, most fibers scored 1 point. Thus, significant differences in the morphology of nerve root fiber were observed between affected and unaffected sides ($P < 0.05$; Figure 2).

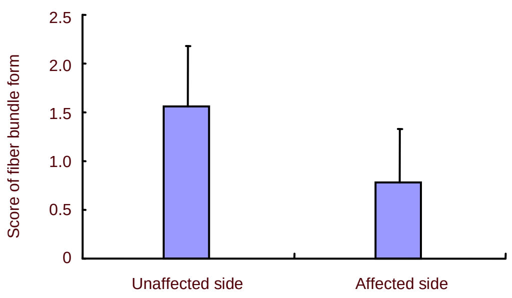

Figure 2 Quantitative comparison of the morphology of nerve roots between affected and unaffected sides in patients with intervertebral disc degeneration-induced radiculopathy.

The morphological score of the nerve roots on the affected side was lower than that on the unaffected side ($P < 0.05$; mean ± SD, $n = 18$, paired t-test).

Fiber-tracking images demonstrated that compressed nerve roots had incomplete fiber bundles, with interrupted fiber bundles in some cases; the morphology of fiber bundles was compact, without branching. Uncompressed nerve roots commonly had intact fiber bundles, with branching (Figure 3).

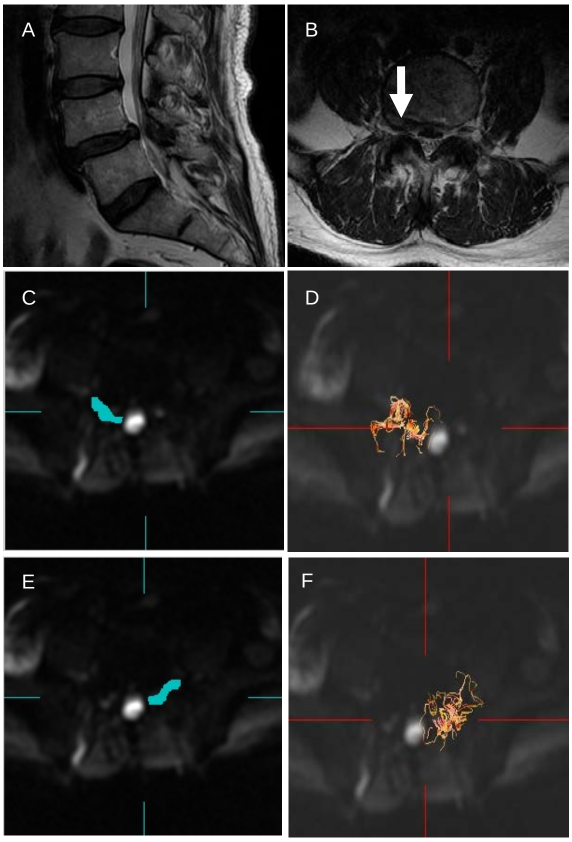

Figure 3 Fiber-tracking images of nerve roots in a 62-year-old female patient with intervertebral disc degeneration-induced radiculopathy.

She presented with right lower limb pain for 1 year. (A) Lumbar sagittal T2-weighted images (T2WI); (B) lumbar $L_{4/5}$ intervertebral disc axial T2WI; (C, E) region of interest for bilateral diffusion tensor tractography; (D, F) cross section of the fiber tracking image of bilateral nerve roots.

$L_{4–5}$ vertebral body slightly slipped; the height of the $L_{4–5}$ intervertebral disc was slightly diminished; loss of high T2 signal, black; intervertebral disc protrusion; the right intervertebral foramen was compacted; nerve roots were compressed; the boundary between the nerve roots and the intervertebral disc was unclear (arrow).

After diffusion tensor tractography, right nerve root fibers gathered together, were incomplete, and the area decreased. The left nerve root fibers were scattered and intact.

DISCUSSION

Radiculopathy is mainly diagnosed by clinical symptoms, but there is no definitive diagnostic criterion[19-21]. Intervertebral disc bulging or protrusion are common causes of radiculopathy, after spondyloarthropathy[22]. It is of important clinical significance to evaluate radiculopathy and guide patient rehabilitation[23-24].

MRI is a frequently used method for examining nerve root morphology. Previous studies have mainly focused on the anatomy of nerve roots in radiculopathy[25-26]. Furthermore, radiculopathy is currently diagnosed mainly based on functional changes of nerve roots. Thus, functional imaging of nerve roots is of great significance for diagnosis, evaluation and treatment of the disease.

The present study first used DT-MRI to conduct functional imaging of spinal nerve roots and investigate radiculopathy induced by intervertebral disc degeneration. Molecular diffusion along the direction of the nerve root was faster than that perpendicular to the nerve root. Thus, molecular diffusion of nerve roots is anisotropic, and diffusion tensor imaging can reveal this characteristic. The sensitivity of diffusion tensor imaging to molecular diffusion is associated with field strength and selected *b* value. The higher the field strength, the bigger the *b* value and the higher the sensitivity.

3.0T MRI was used to elevate the sensitivity of images. The choice of *b* value requires careful consideration. Excessively high *b* values lead to a reduction in signal-to-noise ratio and difficulty in describing a region of interest. If the *b* value is excessively low, images can be impacted by capillary blood flow[27-28]. After multiple pilot experiments, 600 s/mm^2 was selected as the *b* value.

On the basis of diffusion tensor imaging, continuous anisotropy of molecular diffusion was visible within consecutive pixels. If this anisotropic continuity was detected, we then conducted fiber tracking[29]. Software is needed to track nerve root fibers using diffusion tensor imaging. There are two kinds of fiber tracking: definite tracking and probable tracking. Because there were only a few spinal nerve roots in the intervertebral foramen, we used Volume one software with definite tracking.

Results of fiber tracking were associated with the choice of region of interest and the fractional anisotropy threshold[30]. The current study optimized and realized post-processing of diffusion tensor imaging for spinal nerve root injury. The intervertebral foramina was considered as the region of interest for fiber tracking, because intervertebral disc bulging or protrusion-induced nerve root compression always appeared in this region.

Results from this study confirmed that this region of interest could noticeably reveal the changes in nerve roots. Fractional anisotropy is a value representing diffusion anisotropy. A high fractional anisotropy shows a strong anisotropic signal. Nevertheless, the measure of fractional anisotropy can be impacted by fiber crossover, and became low in the region where fiber crossover appeared. The software could track the fiber bundles irrelevant to anatomy or stop tracking. During fiber tracking, a certain fractional anisotropy threshold should be set. That is, tracking ceased when the fractional anisotropy value fell below the threshold. Because no study concerning nerve root fiber tracking has been previously published, this study was performed according to the conditions used for brain fiber tracking with a threshold of 0.18. Experimental results verified that this threshold was effective.

This study summarized a quantitative evaluation system for nerve root injury, which could quantitatively analyze the cross-sectional area of nerve root fibers and their anatomical form to determine nerve root function. Results demonstrated that no significant difference was detected in the number of fiber bundles between affected and unaffected nerve roots. The number of fiber bundles was confined by drawing a region of interest and the size of imaging voxels, and did not represent the real number of nerve roots. The diameter of nerve fibers was far smaller than the pixel area; present magnetic resonance images cannot reveal at the micron level. Moreover, displayed fiber bundles were imaged based on maximum vector. Therefore, the number of fiber bundles was not equal to the number of nerve roots. However, this tracking imaging reflected the real condition of nerve roots to a certain degree by calculating the cross-sectional area of the fiber bundle and by evaluating the morphology of fiber bundles. The cross-sectional area of nerve root fibers on the affected side decreased, which was consistent with what was expected.

It is assumed that bulging or protruding intervertebral discs occupied the intervertebral foramen, and nerve roots were compressed. Morphological observation demonstrated that compressed nerve roots were often gathered, with no branching, and fiber bundles were broken, suggesting that intervertebral disc degeneration resulted in molecular diffusion of nerve roots, and impacted nerve root function. Fiber bundles on the unaffected side were scattered, with natural branching, which was identical to healthy anatomical images.

This study confirmed that some unaffected nerve roots do not present clear branches, but exhibit gathered morphologies, which could be induced by the different scanning slice chosen. If the pedicles of the vertebral arch are located in the central slice within the scanning range, the tracking of fiber bundles in the lateral intervertebral foramen would be impacted. In addition, different vertebral heights of different individuals impacted the presentation of fiber images. To avoid this type of bias, the present study only included patients with unilateral nerve root compression for paired design. Differences in nerve root function could possibly be associated with age and smoking[31]. Because of the finite sample size, the subjects were not grouped according to age.

Future studies will evaluate nerve roots according to different ages. The cross-sectional area of the nerve root was minute and the fractional anisotropy value of molecular diffusion of the nerve roots could not be precisely measured. With the development of hardware for magnetic resonance, MRI images with minute voxels could be obtained. Following this, nerve root function will be better quantified, and the real condition of the nerve root will be displayed, which could be used as a diagnostic tool for radiculopathy. This study cannot establish a diagnostic criterion for radiculopathy using diffusion tensor tractography as the sample size was too limited, but it has implications for the diagnosis of radiculopathy from clinical symptoms.

In summary, this study was the first to use diffusion tensor tractography to reveal spinal nerve root function, which may provide useful for gaining a better understanding of radiculopathy. Diffusion tensor tractography provides useful information on molecular diffusion of spinal nerve roots at the molecular level, along with patient diagnosis, treatment and prognosis.

SUBJECTS AND METHODS

Design

Self-control, imaging experiment.

Time and setting

Experiments were performed in the Department of Medical Imaging, the Second Hospital of Hebei Medical University, China from January to December 2012.

Subjects

A total of 18 patients with intervertebral disc degeneration-induced radiculopathy from the Hebei Province of China were enrolled in this study.
The subjects were diagnosed in accordance with one of the following symptoms: MRI showing reduced T2 signal; intervertebral disc exceeding the vertebral edge; reduction or collapse of intervertebral disc height.

Inclusion criteria: (1) lower back pain and/or lower limb pain, with or without lower limb disorder; (2) intervertebral disc degeneration observed by MRI; (3) intervertebral disc bulging or protrusion caused by unilateral nerve root compression on that plane; (4) nerve root compression by the intervertebral disc or nerve roots showing thin and flat form, having an unclear boundary with the intervertebral disc; (5) without other spinal diseases.

Exclusion criteria: (1) the subjects suffered from other lumbar diseases besides spinal degeneration; (2) a history of trauma; (3) intervertebral disc bulging or protrusion leading to bilateral nerve root compression.

The protocols were conducted in accordance with *Administrative Regulations on Medical Institution*, formulated by State Council of China[32]. The subjects gave informed consent.

Methods

MRI

This study used Signal Excite HD 3.0 T high field-strength MR scanner (GE Healthcare, Fairfield, CT, USA), spine coil. The subjects lay in the supine position, their ears were tightly plugged with cotton wool and they were breathing smoothly. The median line of the body was located in the center of the coil. The long axis of the body was parallel to the long axis of the main field. Scanning sequence included sagittal T1WI, sagittal and axial T2WI and axial diffusion tensor imaging.

The parameters of diffusion tensor imaging were as follows: single shot-spin echo planar imaging sequence, repetition time/echo time: 2 300/75.5 ms, slice thickness 5 mm, no spacing, 256 × 256 matrix, field of view: 38 mm × 38 mm, b value: 0 and 600 s/mm^2, six directions. Sagittal T1WI parameters: repetition time 3 294 ms, echo time 25.4 ms; sagittal T2WI parameters: repetition time 2 500 ms, echo time 108.9 ms; axial T2WI parameters: repetition time 2 440 ms, echo time 120.8 ms.

Data processing

As exhibited in T2WI images (Figures 1, 2), unilateral nerve root compression induced by lumbar degeneration and intervertebral disc bulging or protrusion was diagnosed. Volume one software was used to reveal fiber images on the computer. The left and right intervertebral foramens were selected as regions of interest, which were symmetric, and their areas were identical.

The number of fiber bundles in the regions of interest was calculated, and fiber-tracking images were obtained. Fiber tracking was stopped when fractional anisotropy was < 0.18. Cross sections of fiber bundles were recorded, and the image was input into CAD software (Zhongwang, Guangzhou, Guangdong Province, China). The image was magnified, and the region of fiber bundle was labeled point by point. The area was calculated. The fiber bundle was graded according to morphology. On the transverse axis, the cross-sectional area of the fiber bundles was measured using CAD software.

Statistical analysis

Measurement data were expressed as mean ± SD, and analyzed using SAS 9.0 software (SAS Institute Inc., Cary, NC, USA). The difference in intergroup mean was compared with paired *t*-test. A value of $P < 0.05$ was considered statistically significant.

Research background: Present studies investigating radiculopathy mainly focus on anatomical imaging. The evaluation of nerve root function is significant to guide clinical studies and applications.

Research frontiers: Some scholars outside of China have used three-dimensional fast imaging employing steady state acquisition of CT and magnetic resonance to examine nerve roots. However, no studies have been published concerning the research and evaluation of spinal nerve injury using diffusion tensor imaging.

Clinical significance: This study was the first to use magnetic resonance diffusion tensor tractography to assess nerve root function, with a scanning pattern and post-processing, and established a scoring system of nerve root morphology to evaluate effects of radiculopathy on nerve root function and injury degree.

Academic terminology: Fractional anisotropy is a scalar value between 0 and 1 that describes the degree of anisotropy of a diffusion process. A value of 0 indicates that diffusion is isotropic, *i.e.*, it is unrestricted (or equally restricted) in all directions. A value of 1 indicates that diffusion occurs only along one axis and is fully restricted along all other directions.

Peer review: This study used diffusion tensor magnetic resonance imaging-based tractography to evaluate radiculopathy. As magnetic resonance imaging does not use radiation, it is a promising tool for establishing a diagnostic criterion for radiculopathy.

REFERENCES

[1] Cherkin D, Eisenberg D, Sherman K, et al. Randomized trial comparing traditional Chinese medical acupuncture, therapeutic massage, and self-care education for chronic low back pain. Arch Intern Med. 2001;161(8):1081-1088.

[2] Yabe Y, Honda M, Hagiwara Y, et al. Thoracic radiculopathy caused by ossification of the ligamentum flavum. Ups J Med Sci. 2013;118(1):54-58.

[3] Ando M, Tamaki T, Kawakami M, et al. Electrophysiological diagnosis using sensory nerve action potential for the intraforaminal and extraforaminal L5 nerve root entrapment. Eur Spine J. 2013;22(4):833-839.

[4] Jarvik JG, Deyo RA. Diagnostic evaluation of low back pain with emphasis on imaging. Ann Intern Med. 2002; 137(7):586-597.

[5] Lateef H, Patel P. What is the role of imaging in acute low back pain. Curr Rev Musculoskelet Med. 2009;2(2):69-73.

[6] Chou R, Qaseem A, Snow V, et al. Diagnosis and treatment of low back pain: a joint clinical practice guideline from the American College of Physicians and the American Pain Society. Ann Intern Med. 2007;147(7):478-491.

[7] Sheehan NJ. Magnetic resonance imaging for low back pain: indications and limitations. Postgrad Med J. 2010;86(10):374-378.

[8] Marinelli NL, Haughton VM, Anderson PA. T2 relaxation times correlated with stage of lumbar intervertebral disk degeneration and patient age. AJNR. 2010;31(7):1278-1282.

[9] Mizrahi O, Sheyn D, Tawackoli W, et al. Nucleus pulposus degeneration alters properties of resident progenitor cells. Spine J. 2013.

[10] Tan Y, Aghdasi BG, Montgomery SR, et al. Kinetic magnetic resonance imaging analysis of lumbar segmental mobility in patients without significant spondylosis. Eur Spine J. 2012;21(12):2673-2679.

[11] Zou J, Yang H, Miyazaki M, et al. Missed lumbar disc herniations diagnosed with kinetic magnetic resonance imaging. Spine (Phila Pa 1976). 2008;33(5):E140-E144.

[12] Cohen SP, Gupta A, Strassels SA, et al. Effect of MRI on treatment results or decision making in patients with lumbosacral radiculopathy referred for epidural steroid injections: a multicenter, randomized controlled trial. Arch Intern Med. 2012;172(2):134-142.

[13] Jensen OK, Nielsen CV, Stengaard-Pedersen K. One-year prognosis in sick-listed low back pain patients with and without radiculopathy. Prognostic factors influencing pain and disability. Spine J. 2010;10(8):659-675.

[14] Lurie JD, Moses RA, Tosteson AN, et al. Magnetic resonance imaging predictors of surgical outcome in patients with lumbar intervertebral disc herniation. Spine (Phila Pa 1976). 2013;38(14):1216-1225

[15] Makarand K. Constructive interference in steady-state/ FIESTA-c clinical applications in neuroimaging. J Med Imaging Radiat Oncol. 2011;55(2):183-190.

[16] Pfirrmann CW, Dora C, Schmid MR, et al. MR image-based grading of lumbar nerve root compromise due

to disk herniation: reliability study with surgical correlation. Radiology. 2004;230(2):583-588.
[17] Zhang Y. Thoracic dorsal root ganglion: an initial study of anatomyand imaging techniques. Nanchong: North Sichuan Medical College. 2011.
[18] Liu CH, Du TQ, Dong J, et al. Clinical application of 2D-FIESTA Cine imaging in the treatment of lumbar disc herniation. Zhongguo Guzhongliu Gubing. 2011;10(1): 39-41.
[19] Shah KC, Rajshekhar V. Reliability of diagnosis of soft cervical disc prolapse using Spurling's test. Br J Neurosurg. 2004;18(5):480-483.
[20] Boswell MV, Shah RV, Everett CR, et al. Interventional techniques in the management of chronic spinal pain: evidence-based practice guidelines. Pain Physician. 2005; 8(1):1-47.
[21] Acosta FL Jr, Ames CP. Cervical disc arthroplasty: general introduction. Neurosurg Clin N Am. 2005;16(4):603-607.
[22] Radhakrishnan K, Litchy WJ, O'Fallon WM, et al. Epidemiology of cervical radiculopathy. A population-based study from Rochester, Minnesota, 1976 through 1990. Brain. 1994;117(2):325-335.
[23] Lin CH, Tsai YH, Chang CH, et al. The Comparison of multiple f-wave variable studies and magnetic resonance imaging examinations in the assessment of cervical radiculopathy. Am J Phys Med Rehabil. 2013.
[24] Ando M, Tamaki T, Kawakami M, et al. Electrophysiological diagnosis using sensory nerve action potential for the intraforaminal and extraforaminal L_5 nerve root entrapment. Eur Spine J. 2013;22(4):833-839.
[25] Rüttimann B. A historical approach to herniated disk. Schweiz Rundsch Med Prax. 1900;79(25):791-796.
[26] Pfirrmann C, Dora C, Schmld M, et al. MR image-based grading of lumbar nerve root compromise due to disk herniation: reliability study with surgical correlation. Radiology. 2004;230(6):583-588.
[27] Kerttula L, Jauhiainen J, Tervonen Osmo, et al. Apparent diffusion coefficient in thoracolumbar intervertebral discs of healthy young volunteers. J Magn Reson Imaging. 2000;12(2):255-260.
[28] Niu G, Yu X, Yang J, et al. Apparent diffusion coefficient in normal and abnormal pattern of intervertebral lumbar discs: initial experience. J Biomed Res. 2011;25(3): 197-203.
[29] Yin YJ, Jiang JW, Jiang LW, et al. 3D FIESTA to assess cauda equina. Zhongguo Wuzhen Yixue Zazhi. 2010;10(3):532-533.
[30] Zhang Y, Wan SH, Wu GJ, et al. Magnetic resonance diffusion tensor imaging and diffusion tensor tractography of human visual pathway. Int J Ophthalmol. 2012;5(4): 452-458.
[31] Desai A, Bekelis K, Ball PA, et al. Spine patient outcomes research trial: do outcomes vary across centers for surgery for lumbar disc herniation? Neurosurgery. 2012;71(4): 833-842.
[32] State Council of the People's Republic of China. Administrative Regulations on Medical Institution. 1994-09-01.

(Reviewed by Wallace M, Pack M, Wang ZC, Yang YM)
(Edited by Wang J, Qiu Y, Li CH, Song LP, Liu WJ, Zhao M)